P.R.L.

TECHNICAL NOTE

TN-82-80

TN-~~82-02~~.
TN82-80

COMPUTER STUDY OF A PHASE SCANNED 56 ELEMENT SBF ARRAY

By

Ramesh Sharma, P. Muralikrishna,
S.K.Shah and P.Venat

June,1982

PHYSICAL RESEARCH LABORATORY
AHMEDABAD

CONTENTS

COMPUTER STUDY OF A PHASE SCANNED 256 ELEMENT SBF ARRAY

Ramesh Sharma, P. Muralikrishna, S.K. Shah and P. Venat

Abstract

As part of the design study of a high power MST Radar, the theoretical radiation pattern of a 256 element phase scanned Short Back Fire (SBF) antenna array was studied in detail using computer software and the results are reported here. The array consists of identical SBF elements arranged in a planar doubly periodic array in a 16 x 16 geometry. The interelement distance is chosen as 1 λ , so that the mutual coupling between the individual SBF elements can be neglected. The effect of introducing differential phase gradients between the SBF elements is also studied in detail, with an ultimate objective of arriving at an upper limit for the antenna beam steerability by the differential phase gradient technique.

Key words:

1) Antenna array
2) Beam tilt angle
3) Grating lobes
4) Phase scanning
5) Visible range

1. Introduction:

The Short Back Fire antenna belongs to a comparatively new class of antennas. This was invented by Hermann E Ehrenspeck of Air Force Cambridge Research Laboratories. A typical Short Back-Fire antenna is shown schematically in Figure (1). It essentially consists of two plane reflectors (R and M) of unequal apertures arranged parallel to each other. A half wave dipole feed is placed midway between the two reflectors and transverse to the axis of the reflectors. A peripheral circular rim of diameter λ is also provided. This rim serves mainly two purposes (a) it reduces backward and side lobes (b) it increases directivity of the antenna by additional contribution from the edge of the rim.

Such a system is characterised by multiple reflections of electromagnetic waves and radiation occurs beyond the smaller of the two reflectors. It can be thought of as a back fire antenna of 0.5 λ length surrounded by a peripheral circular rim, of diameter λ .

The radiation pattern of an SBF antenna array consisting of 256 elements arranged in 16 rows of 16 elements each in a plane is studied in detail using computer software. Consecutive elements in a row are separated by a distance λ .

Adjacent rows are also separated by distance of λ . The beam steerability of such an array by introducing differential phase gradients between the adjacent radiating elements is studied in detail with an aim to electronically scan the radiation pattern of the array in free space. Beam steerability is limited by the appearance of what are known as grating lobes and beam steering beyond a particular angle becomes impossible.

2. Theoretical Formulation:

The radiation pattern of a finite sized phased array is expressed as the product of the array of factor and the radiation pattern of the single radiation element.

A rectangular co-ordinate system shown in Figure (2) is used here to represent the array and the far field radiation pattern. P is an observation point in the far field of the array. r is the distance of P from the origin of the co-ordinate system. The far-field region of an array begins where the angular field distribution is practically independent of the distance of the point from the antenna. For an antenna array which is located near the origin and whose largest dimension D is much larger than the wavelength of the radiation field, the far field is usually assumed to exist at $r \geq \frac{2D^2}{\lambda}$.

Consider a linear array of M isotropic radiators with an inter-element spacing of d wavelengths along the X axis. The first element is assumed to be at the origin. The magnitude of the total transverse electric field strength at the far field point P is given by

$$E_P = \left| \sum_{M=0}^{M-1} E_m \, e^{j\,mkd\cos\theta_x} \right| \qquad \ldots(1)$$

where

E_m is the complex value of the field produced by the m^{th} element and is therefore proportional to the current in that element. The complex nature of E_m accounts for the phase shifts between the currents in the elements.

and k is the free space phase constant (wave number equal to $2\pi/\lambda$). Differences in the path length from each element to P are equal to $mkd \cos \theta_x$.

The absolute value of E normalised to E_o and the number of elements is called the array space factor and is given by

$$S_x = \frac{1}{M} \left| \sum_{m=o}^{M-1} A_m \, e^{j\,mkd\cos\theta_x} \right| \qquad \ldots(2)$$

where $A_m = E_m/E_o$

Similarly the corresponding space factor for N isotropic radiators along the y axis is given by

$$S_y = \frac{1}{N} \left| \sum_{n=o}^{N-1} A_n \, e^{jnkd\cos\theta_y} \right| \qquad \ldots(3)$$

Plotting the space factor as a function of polar angles θ_x and θ_y yields a normalised field strength pattern for the array (Schelkunoff and Friss, 1955).

A special case of the linear array is the uniform linear array where each element has the same current magnitude and therefore produces the same field intensity. Phase shifts are uniform from one element to the next. The current in the m^{th} element along x axis leads the current in the $(m-1)^{th}$ element by δ_x.

Case (i) $\delta_x = 0$: This is the case when all currents are in phase. In this case the maximum in the radiation pattern or the main lobe is perpendicular to the x-axis. This can be denoted by writing $\theta_{xm} = \pi/2$.

Case (ii) $\delta_x \neq 0$: A nonzero value of δ_x causes the main lobe to be located at some other position. In this case θ_{xm} is given by

$$kd \cos \theta_{xm} = -\delta_x \qquad \ldots(4)$$

Applying equation (2) to a uniform array along the x-axis with $A_m = 1$, and replacing the term mkd Cos θ_x by $m\psi_x$ one can get (Weeks, 1968) an expression for the space factor S_x as,

$$S_x = \frac{1}{M} \left| \sum_{m=0}^{M-1} e^{jm\psi_x} \right| \qquad \ldots (5)$$

where $\psi_x = kd \cos \theta_x + \delta_x$ $\qquad \ldots (6)$

The assummation in equation (5) is recognized as a geometric series and can be simplified as

$$S_x = \frac{1}{M} \left| e^{j(M-1)\psi_x} \frac{\sin(M\psi_x/2)}{\sin \psi_x/2} \right| \qquad \ldots (7)$$

Equation (7) is obtained under the assumption that the origin coincides with the first antenna element. Alternately the origin may be placed at the center of the array. If the number of elements in the array is odd, then the central element may be called the 0^{th} element and the array factor written in the form

$$S_x = \frac{1}{M} \left| \sum_{m=-\frac{(M-1)}{2}}^{\frac{(M-1)}{2}} e^{jm\psi_x} \right|$$

Here also the summation is a geometric series with the first term equal to $e^{-j\frac{(M-1)}{2}\psi_x}$. The summation in this case gives,

$$S_x = \frac{1}{M}\left|\frac{\text{Sin}\,\frac{M}{2}\psi_x}{\text{Sin}\,\psi_{x/2}}\right| \qquad \ldots(8)$$

This equation, which physically represents the same array as equation (7) shows that the phase factor $e^{j\frac{(M-1)}{2}\psi_x}$ in equation (7) arises because of the initial choice of the origin at the end of the array. This phase factor disappears when the origin is taken at the center and hence is not usually of fundamental concern.

If the number of elements in the array is even, the placement of the origin at the center of the array requires some additional manipulation since the distance from the origin to the nearest elements is then d/2. But it can be easily shown that the summation in this case also is effectively same as that given by equation (8).

$$S_y = \frac{1}{N}\left|\frac{\text{Sin}\,\frac{N\,\psi_y}{2}}{\text{Sin}\,\psi_{y/2}}\right| \qquad \ldots(9)$$

where $\psi_y = kd \cos \theta_y + \delta_y$ ...(10)

and $\delta_y = -kd \cos \theta_{ym}$ ...(11)

When the radiating elements in array are non isotropic, the pattern of each radiator must be included in the total antenna pattern. The principle of pattern multiplication states that the total antenna pattern equals the product of the element pattern and the array pattern. For example, the space factor for a uniform M x N planar array is

$$S_{xy} = S_x S_y = \frac{1}{M} \left| \frac{\sin \frac{M\psi_x}{2}}{\sin \psi_{x/2}} \right| \frac{1}{N} \left| \frac{\sin \frac{N\psi_y}{2}}{\sin \psi_{y/2}} \right| \quad \ldots(12)$$

The total radiation pattern is obtained by multiplying the pattern derived from (12) by the element pattern (Kraus, 1950).

16 x 16 SBF Array:

If the present case of 16 x 16 BF array, using equations (8) and (9) we get

$$S_x = \frac{1}{16} \left| \frac{\sin 8\psi'_x}{\sin \psi_{x/2}} \right| \quad \ldots(13)$$

and $$S_y = \frac{1}{16} \left| \frac{\sin 8\psi_y}{\sin \psi_{y/2}} \right| \qquad \ldots(14)$$

S_x and S_y are identical periodic functions of ψ_x and ψ_y respectively. A rectangular plot of S_x versus ψ_x is shown in Figure (3).

To obtain the total antenna beam pattern, the space factor S_{xy} has to be multiplied by the radiation pattern of the SBF element. The SBF antenna pattern used in the present case is the theoretical pattern reported by Patel (1971) shown in Fig. (4). The H-plane ($\theta_x = \pi/2$ plane) pattern for the 16 x 16 SBF array is given by:

$$P_{aH} = \left| P_H(\theta_y) \frac{1}{16} \cdot \frac{\sin 8\psi_x}{\sin \psi_{x/2}} \cdot \frac{1}{16} \cdot \frac{\sin 8\psi_y}{\sin \psi_{y/2}} \right| \qquad \ldots(15)$$

Where $P_H(\theta_y)$ is the field intensity pattern of a single SBF element shown in Figure (4). The E plane ($\theta_y = \pi/2$ plane) pattern for the array is obtained by multiplying the H-plane array pattern by the dipole radiation factor $D(\theta_x)$

$$D(\theta_x) = \left| \frac{\cos(\pi/2 \cos \theta_x)}{\sin \theta_x} \right| \qquad \ldots(16)$$

4. Phase Scanning:

To scan the antenna array beam electronically, progressi phase shifts are introduced in adjacent elements as shown in Figure (5). The incremental progressive phase shift is related to the beam tilt angle through the relation given below:

$$\delta_x = \frac{2\pi d}{\lambda} \sin \theta_x \qquad \ldots (17)$$

where δ_x is the incremental phase shift introduced in the elements along the x axis.

and θ_{Tx} is the beam tilt angle in x-z plane measured from the vertical.

Similar relationship is used to obtain the incremental phase shifts for tilting the beam in the y-z plane. For a vertically directed beam δ_x and δ_y are zero as can be seen from the above relationship. The beam tilt angle θ_{Tx} and the corresponding values of δ_x for selected θ_{Tx} values are given in Table 1.

5. Grating lobe:

In the rectangular plot of S_x versus ψ_x (shown in Figure (3)) it can be seen that S_x exists for all values of ψ_x. However the only values of S_x which contribute

to the polar plot of the array radiation pattern are those which correspond to ψ_x values between $-(kd + \delta_x)$ and $(kd + \delta_x)$. This range of ψ_x is generally known as the "visible" range. If the visible range indicates the principal maximum of the antenna beam, and a few secondary maxima, the main lobe of the radiation pattern will be rather broad with a few broad side lobes. When the visible range is enlarged by increasing the value of d, (the interelement separation) more side lobes start appearing, and the individual lobes start narrowing down somewhat. But when d is increased further another principal maxima at ψ_x values $\pm 2\pi$, $\pm 4\pi$ etc. appear within the visible range. These are generally known as grating lobes. The maximum beam tilt angle achievable in an array by the incremental phase shift method is limited by the appearance of grating lobes in the visible range.

6. Results and Discussion:

The radiation pattern for the 256 element SBF array arranged in 16 x 16 geometry is obtained using equation (15) in the E plane. This is shown in Figure (6). Using the incremental phase shift δ_x values corresponding to selected θ_{Tx} values given in Table (1), the radiation field pattern were again obtained for various beam tilts. These are shown in Figures (7) to (13).

As can be seen from Figure (6), the broad side beam has a half power beam width of about 3°, in the E plane. The maximum side lobe level is -14 db below the principal maximum.

A close examination of Figures (6) to (11) shows that the maximum side lobe level though remains unaltered in its absolute value, it increases in relation to the principal maximum from a value of about -14 db for 0° beam tilt to -12 db for 22° beam tilt. For beam tilts greater than 22°, the grating lobe starts appearing in the visible range, and starts dominating over the side lobes. For a beam tilt of 25° the grating lobe level is only -7 db below the principal maximum and it continuously increases further and for a beam tilt of 30°, what one obtains is two lobes of equal power level.

7. Conclusion:

In conclusion one could say that, the 16 x 16 SBF array can give a half power beamwidth of about 3° in both E and H planes, with a maximum side lobe level of about -14 db below the principal maximum. The maximum advisable tilt angle, by phase scanning method is about 22°, at which the grating lobes level becomes equal to the maximum side lobe level. It should be noted here that in the present estimates, only

the main lobe of the single SBF element is considered and the effect of side lobes are neglected. However, in an array the main parameters such as the half power beam width and the side lobe level are mainly decided by the space factor and not by the radiation pattern of the elements in the array.

Acknowledgements

The authors gratefully acknowledge the keen interest shown by Prof. R.V. Bhonsle, in the studies reported here. We would like to thank Mr. D. Stephen for the neat typing of this technical note.

References

1. Schelkunoff, S.A. and H.T. Friss, Antenna Theory and Practice, Wiley, New York, 1952.

2. Weeks, W.L., Antenna Engineering, McGraw-Hill, New York, 1968.

3. Kraus, J.D., Antennas, McGraw-Hill, New York, 1950.

4. Patel, D.C., Short backfire antenna far field radiation pattern, Int. J. Electronics, 30, No.2, 185, 1971.

Table 1: Beam tilt angle and corresponding differential phase shift

Sr. No.	Beam tilt angle (θ_{Tx} deg.)	differential phase shift (δ_x radians)
1.	10	1.09
2.	15	1.63
3.	20	2.149
4.	21	2.25
5.	22	2.354
6.	25	2.655
7.	30	3.142

Figure Captions

Fig.1 : Schematic of a single element short back fire (SBF) antenna.

Fig.2 : Co-ordinate system.

Fig.3 : Variation of the array space factor in the X-direction (S_x) versus ψ_x, for a 16 x 16 SBF array for zero beam tilt.

Fig.4 : Theoretical radiation pattern of a single SBF antenna in the H-plane.

Fig.5 : Beam tilting by introducing progressive phase shifts.

Fig.6 : Normalised radiation pattern of a 16 x 16 SBF array in the E-plane for beam tilt angle = 0°.

Fig.7 : Normalised radiation pattern of a 16 x 16 SBF array in the E-plane for beam tilt angle = 10°.

Fig.8 : Normalised radiation pattern of a 16 x 16 SBF array in the E-plane for beam tilt angle = 15°.

Fig.9 : Normalised radiation pattern of a 16 x 16 SBF array in the E-plane for beam tilt angle = 20°.

Fig.10: Normalised radiation pattern of a 16 x 16 SBF array in the E-plane for beam tilt angle = 21°.

Fig.11: Normalised radiation pattern of a 16 x 16 SBF array in the E-plane for beam tilt angle = 22°.

Fig. 12 : Normalised radiation pattern of a 16 x 16 SBF array in the E-plane for beam tilt angle = 25°.

Fig. 13 : Normalised radiation pattern of a 16 x 16 SBF array in the E-plane for beam tilt angle = 30°.

SINGLE ELEMENT SHORT BACK FIRE ANTENNA

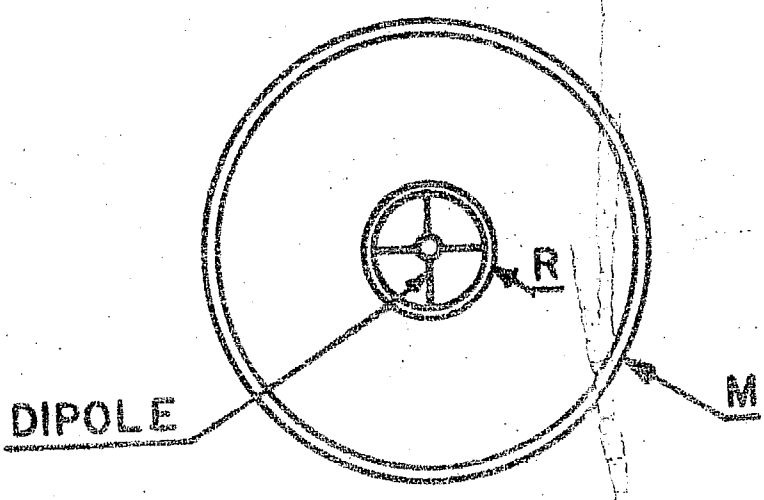

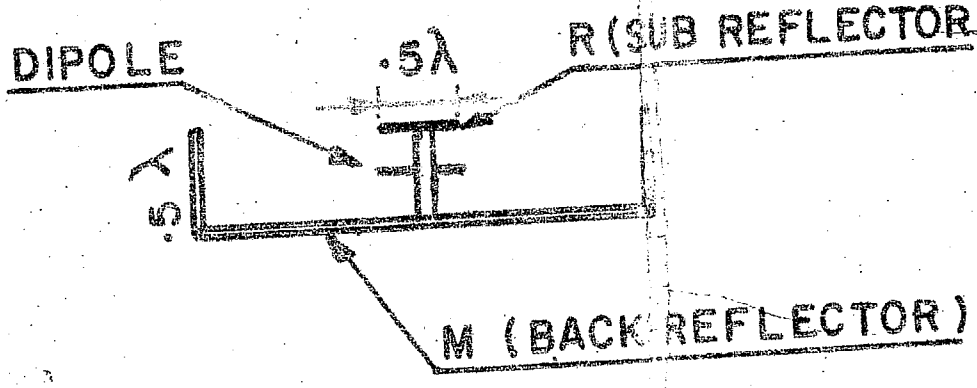

Fig. 1: Schematic of a single element short back fire (SBF) antenna.

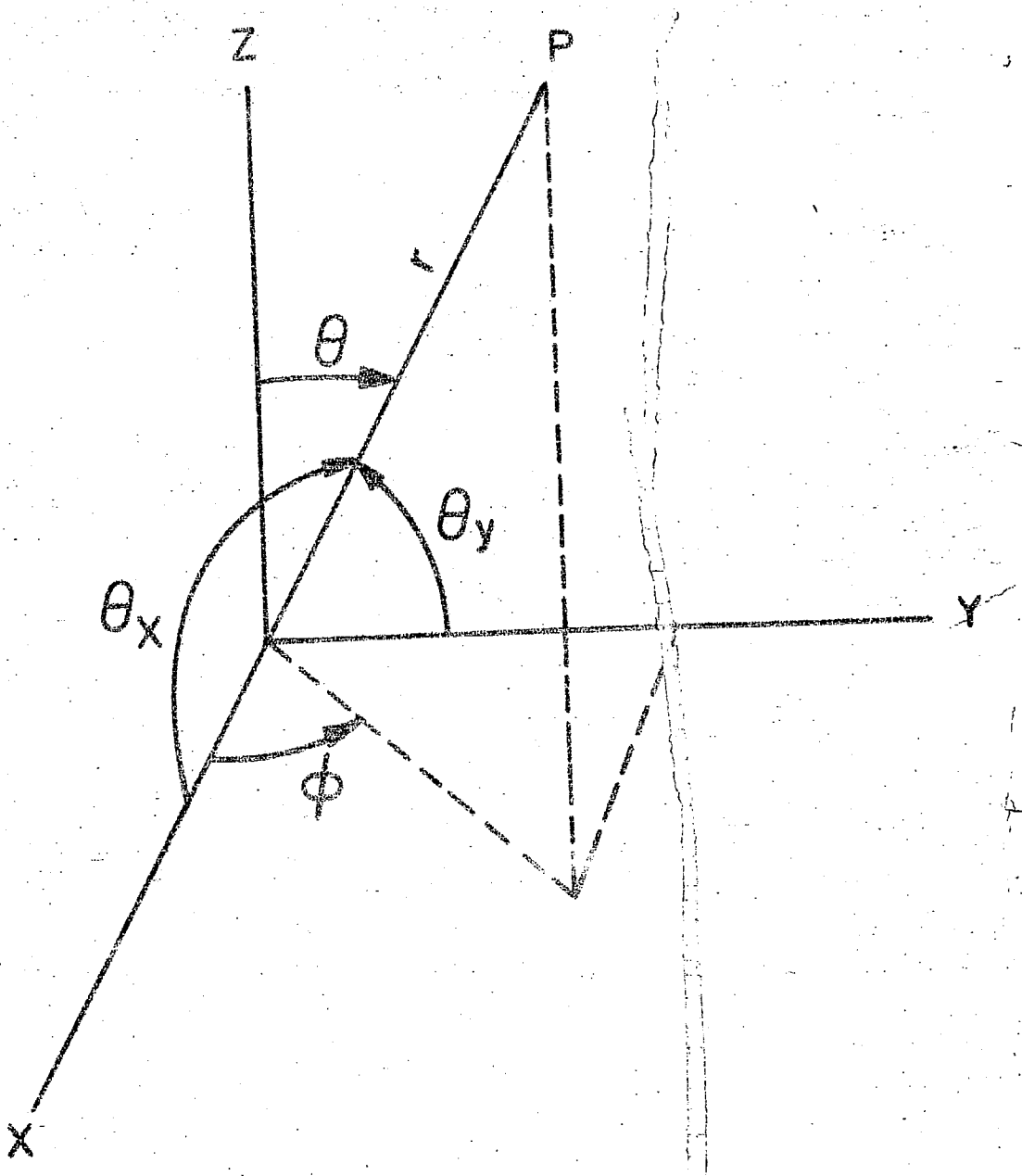

FIG.2. CO-ORDINATE SYSTEM

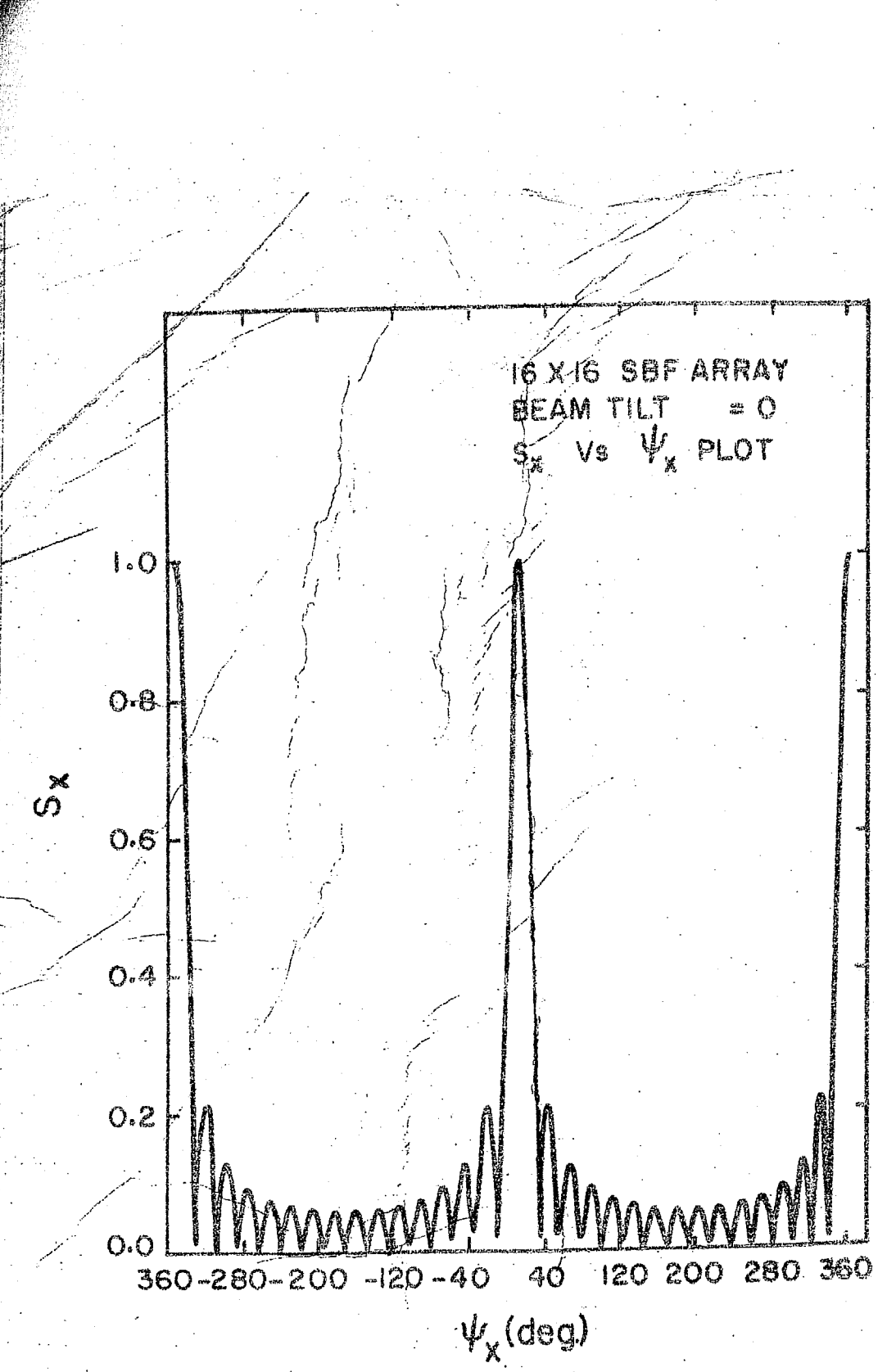
16 X 16 SBF ARRAY
BEAM TILT = 0
S_x Vs ψ_x PLOT
1.0
0.8
0.6
0.4
0.2
0.0
S_x
360 -280 -200 -120 -40 40 120 200 280 360
ψ_x (deg.)

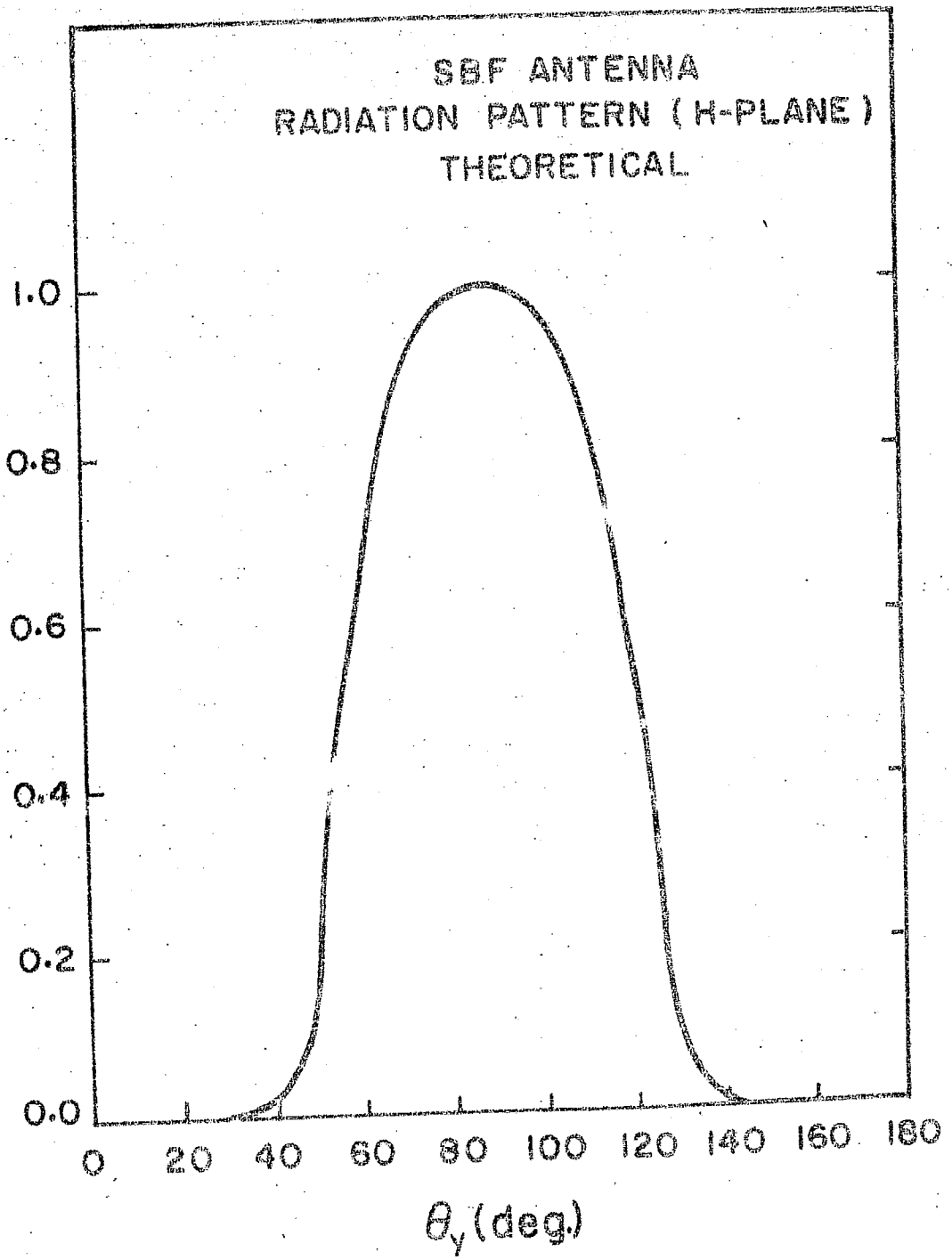

Fig. 4: Theoretical radiation pattern of a single SBF antenna in the H-plane.

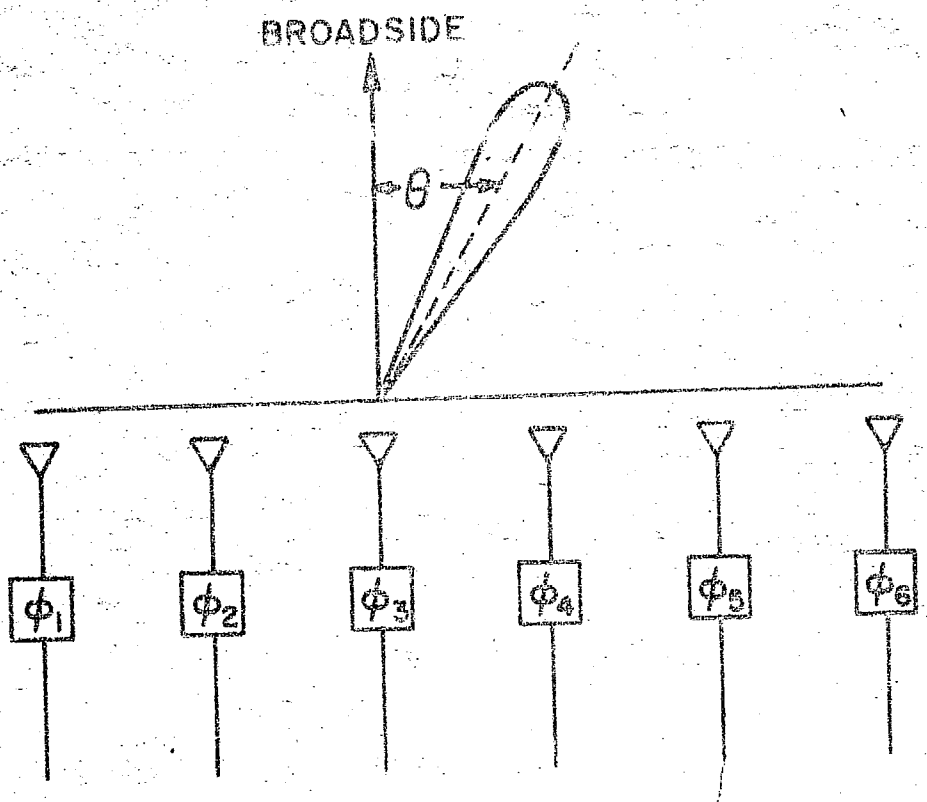

$\theta = \sin^{-1} \frac{\delta\lambda}{2\pi d}$ IS THE BEAM TILT ANGLE RELATIVE TO BROAD SIDE

$\delta = \phi_2 - \phi_1 = \phi_3 - \phi_2 = \phi_4 - \phi_3$ = IS THE DIFFERENTIAL PHASE SHIFT

d = INTER ELEMENT SPACING

λ = FREE SPACE WAVELENGTH

FIG. 5 : BEAM TILTING BY INTRODUCING PROGRESSIVE PHASE SHIFTS

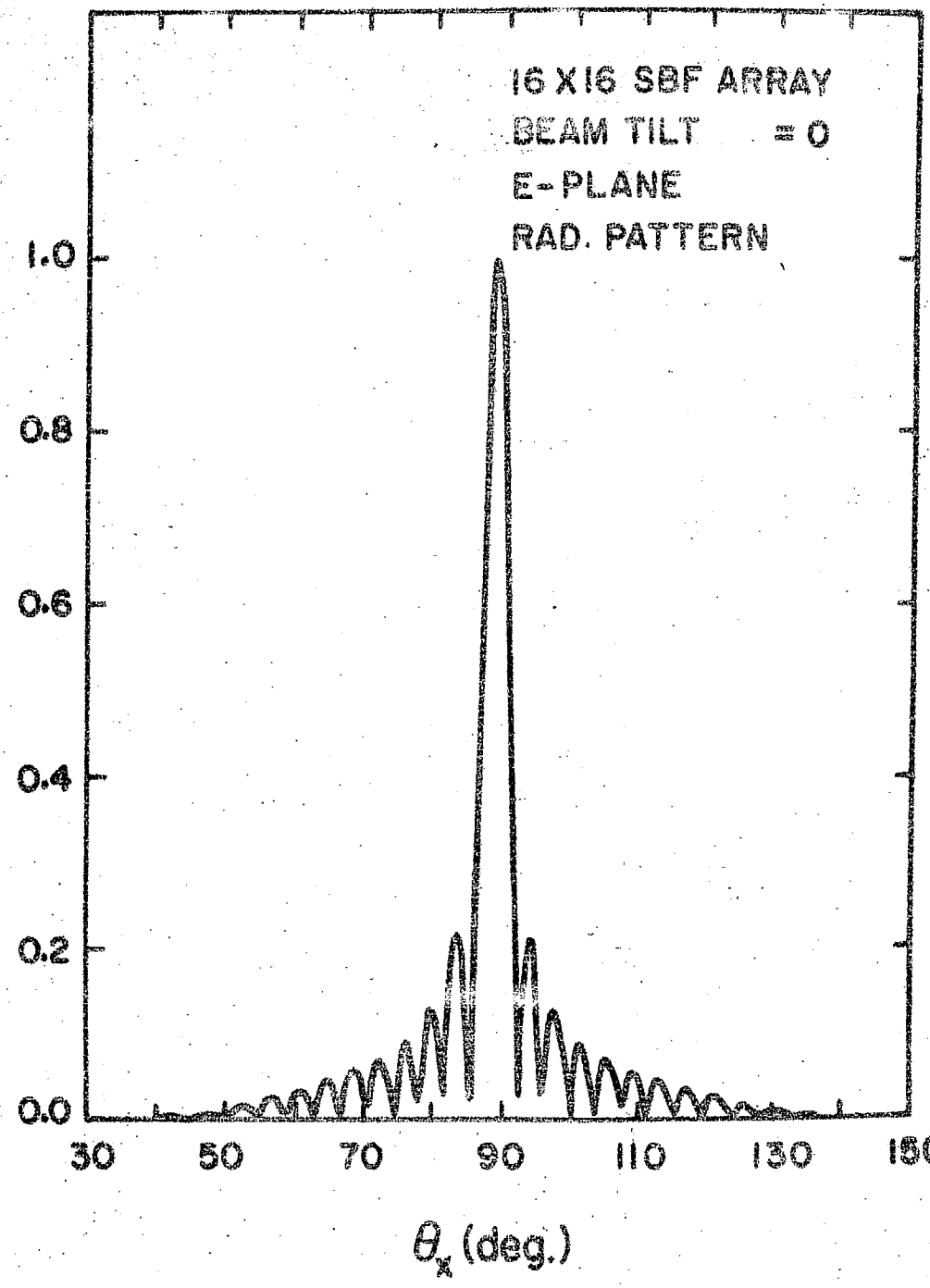

Fig. 6: Normalised radiation pattern of a 16 x 16 SBF array in the E-plane for beam tilt angle = 0^0.

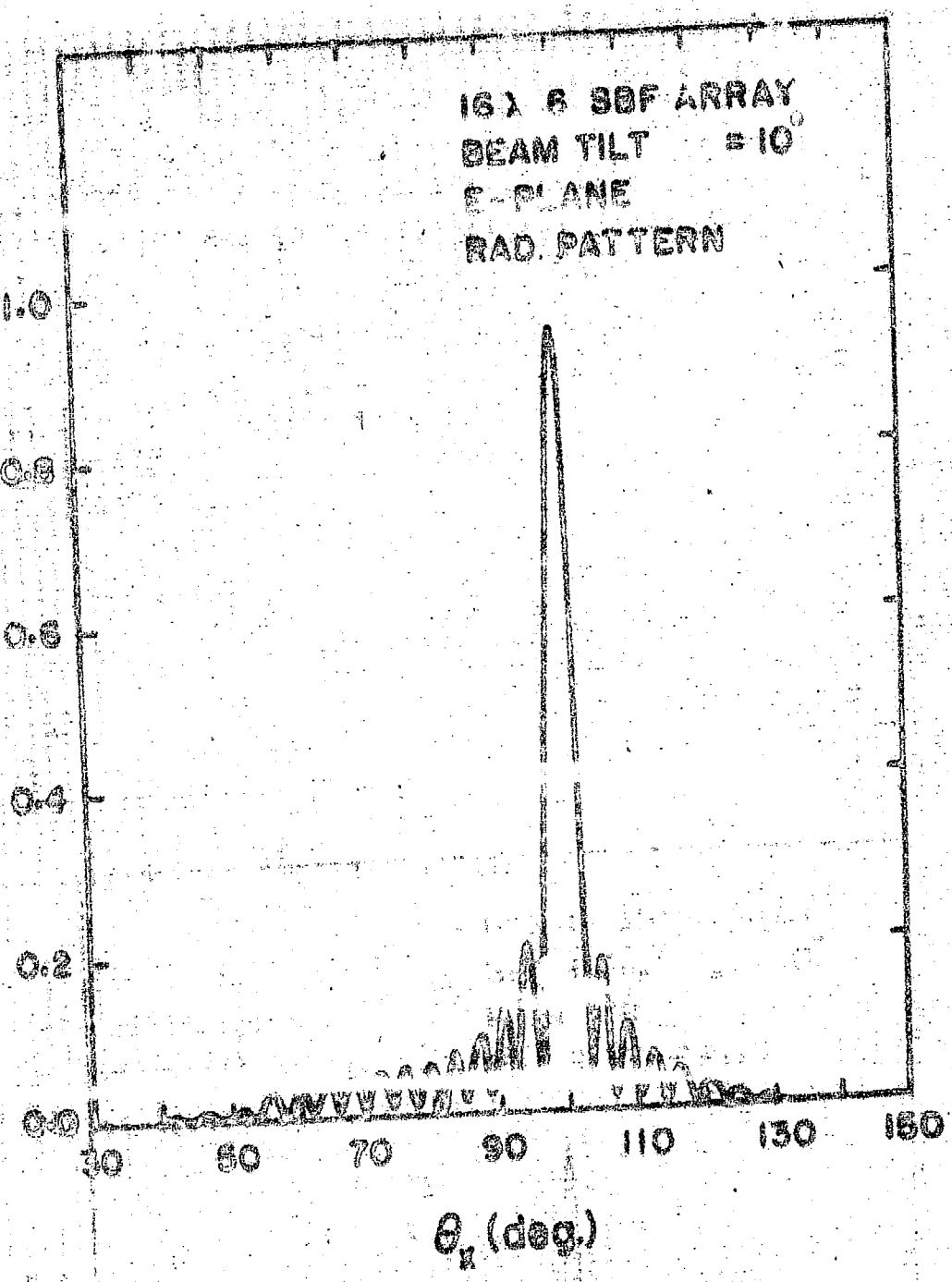

Fig. 7: Normalized radiation pattern of a 16 x 16 SBF array in the E-plane for beam tilt angle = 10°.

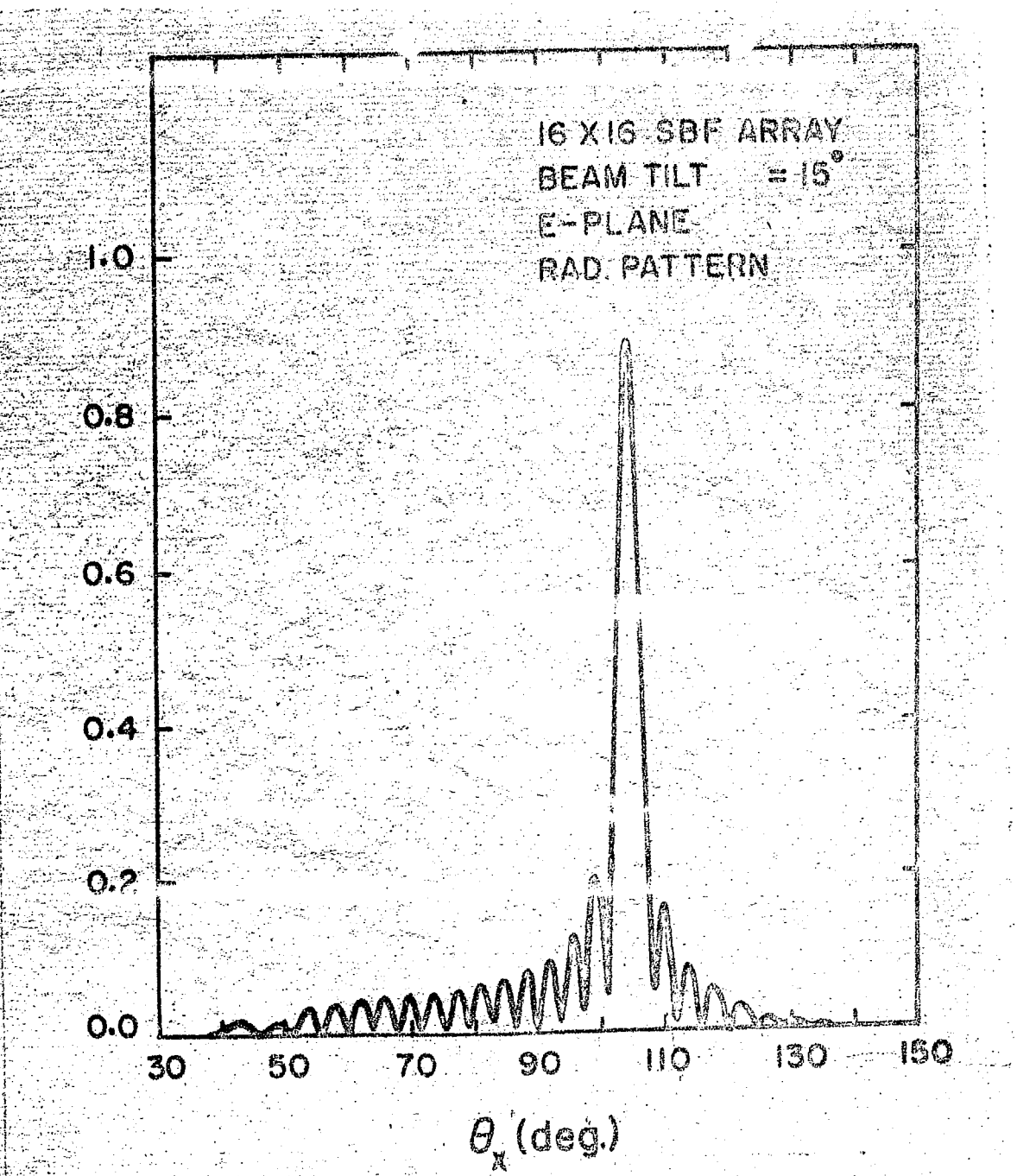

Fig. 8: Normalised radiation pattern of a 16 x 16 SBF array in the E-plane for beam tilt angle = 15°

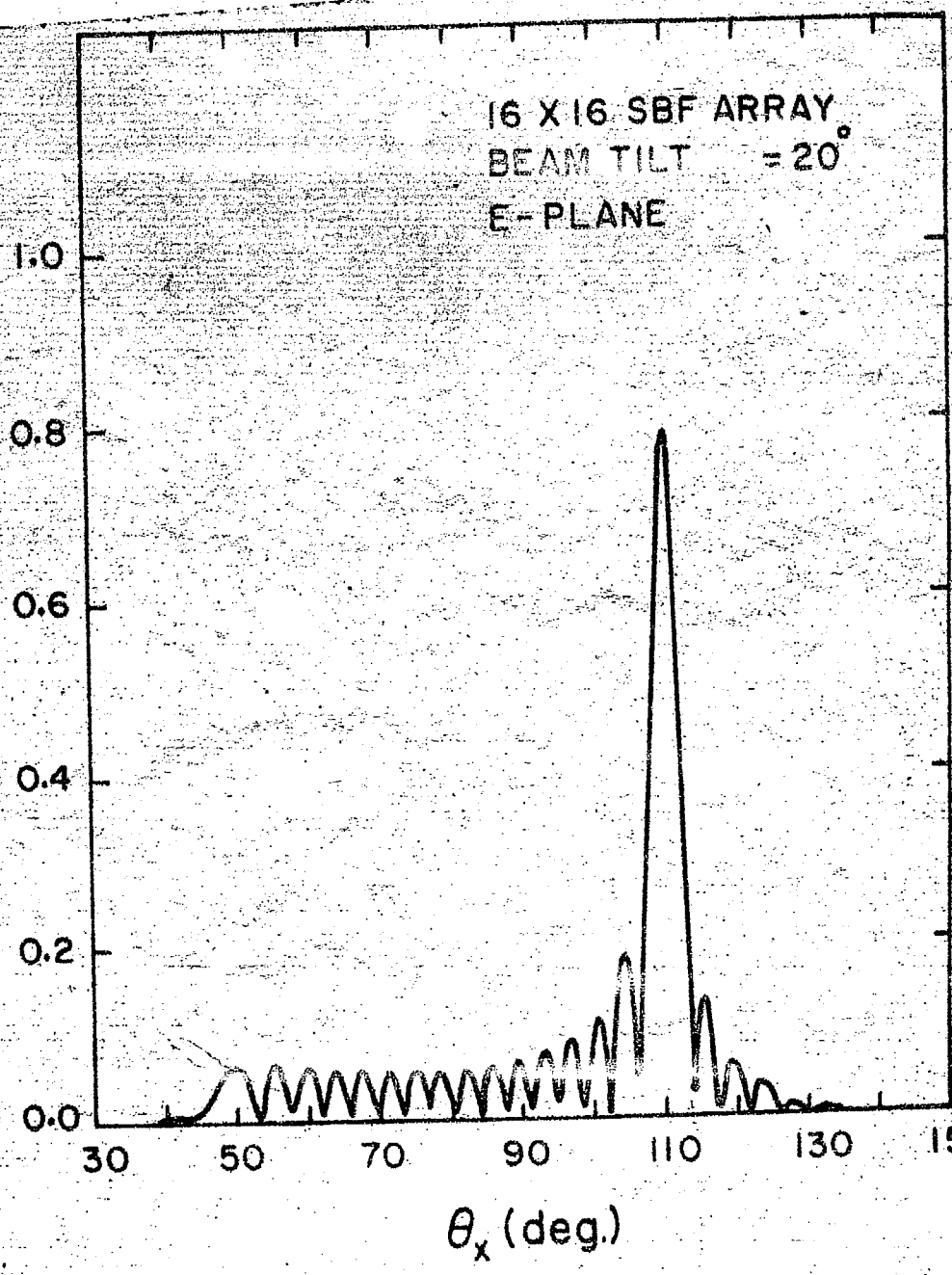

Fig. 9: Normalised radiation pattern of a 16 x 16 SBF array in the E-plane for beam tilt angle = 20°.

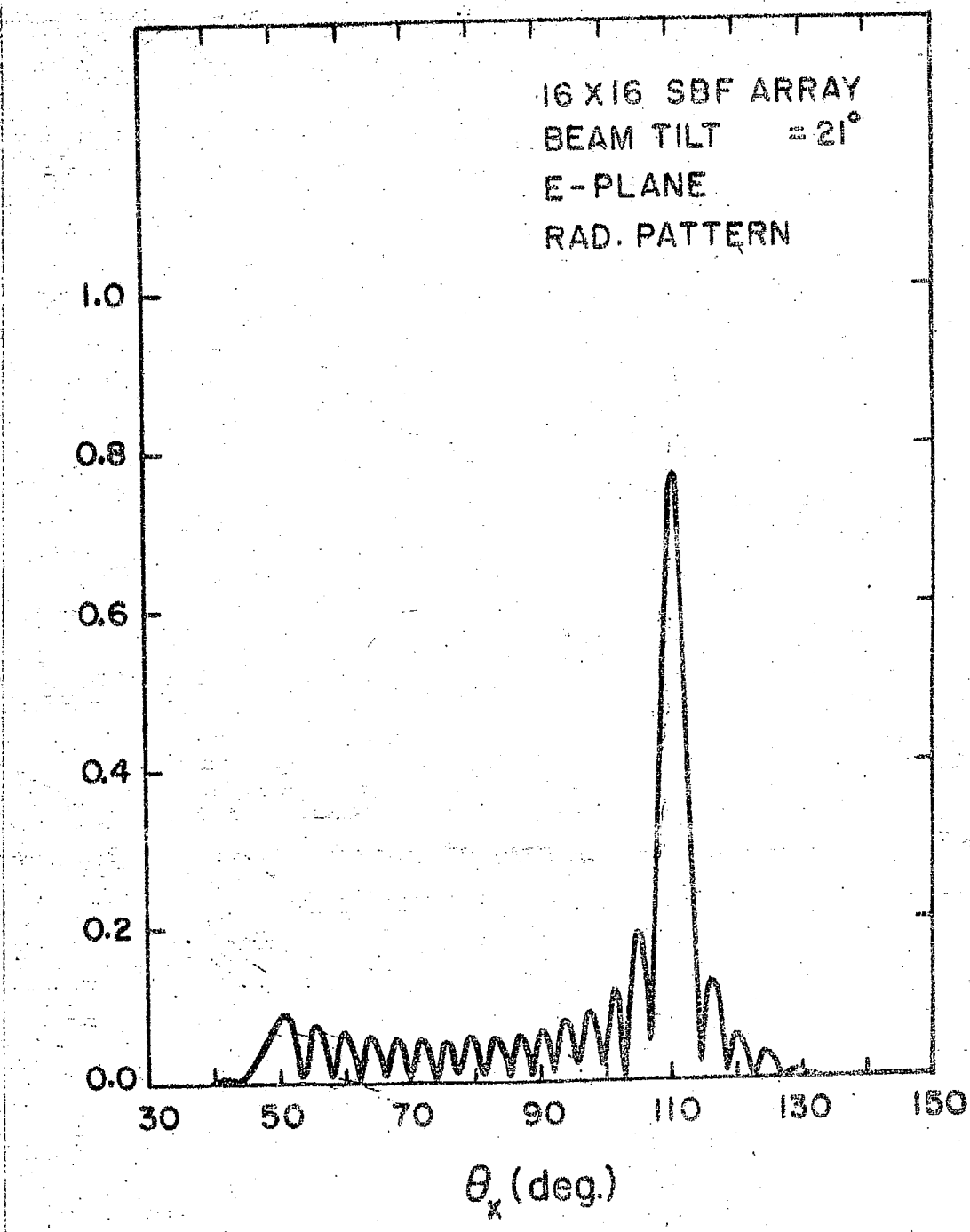

Fig. 10: Normalised radiation pattern of a 16 x 16 SBF array in the E-plane for beam tilt angle = 21°.

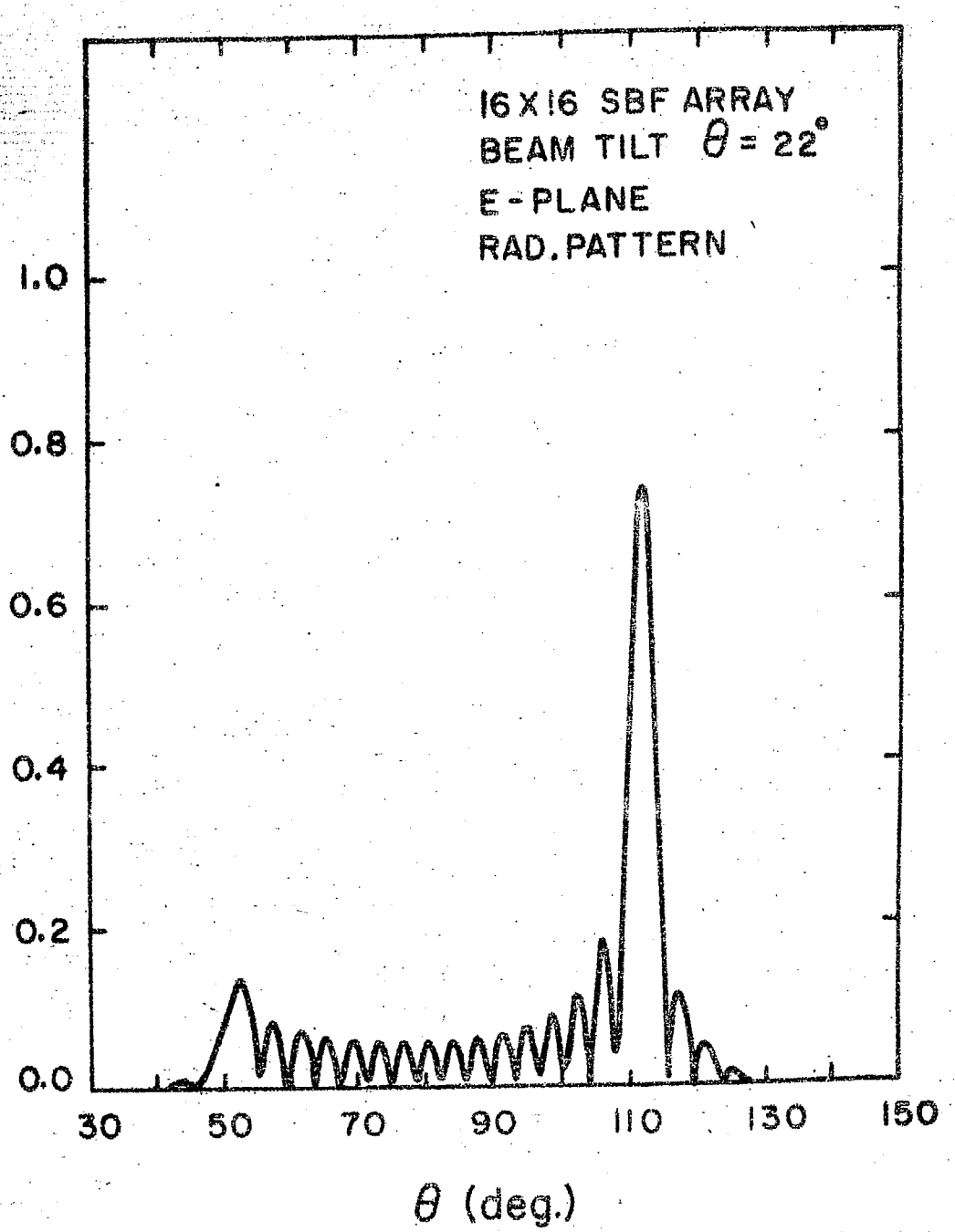

Fig. 11: Normalised radiation pattern of a 16 x 16 SBF array in the E-plane for beam tilt angle = 22°.

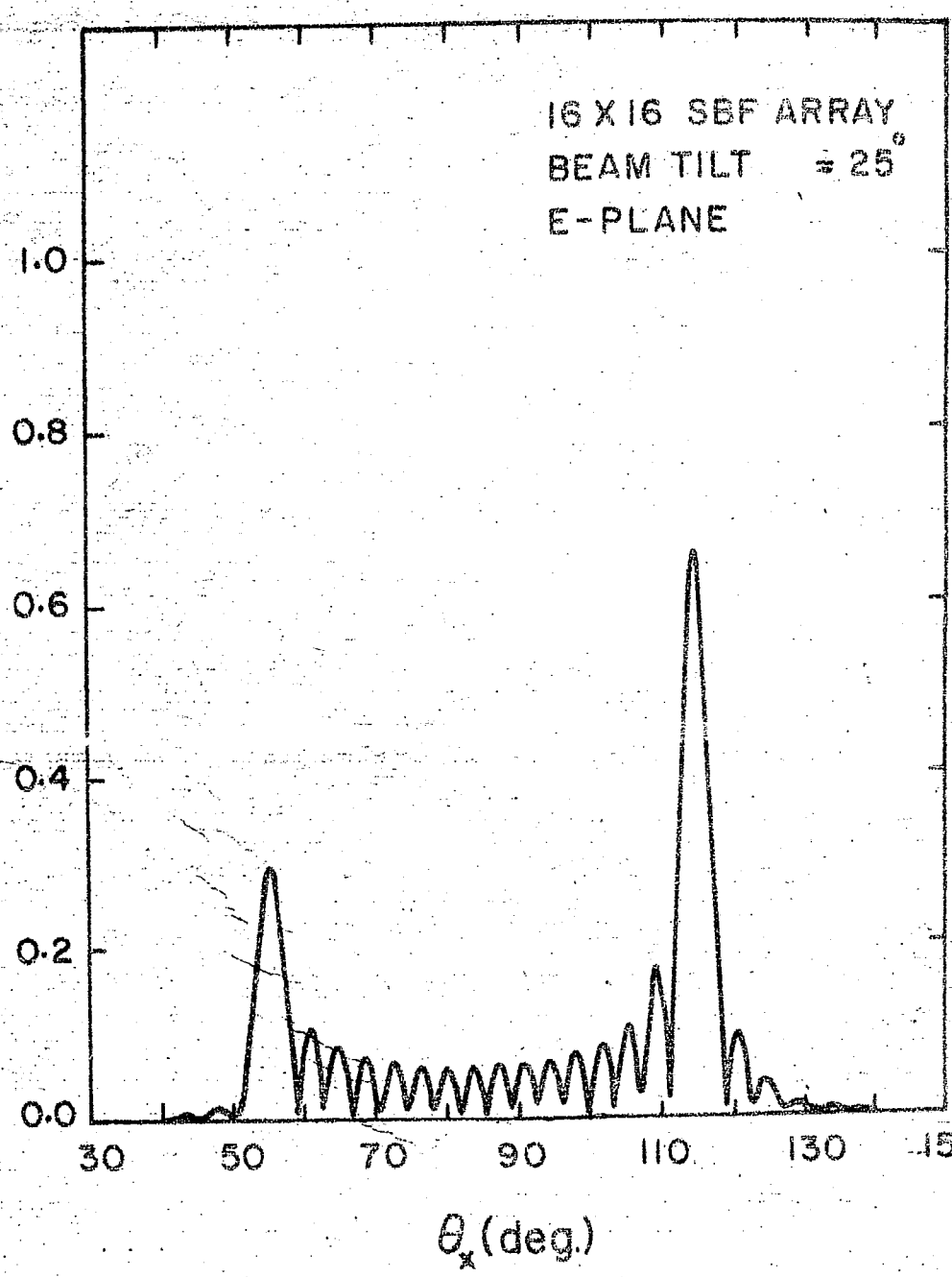

Fig. 12: Normalised radiation pattern of a 16 x 16 SBF array in the E-plane for beam tilt angle = 25°

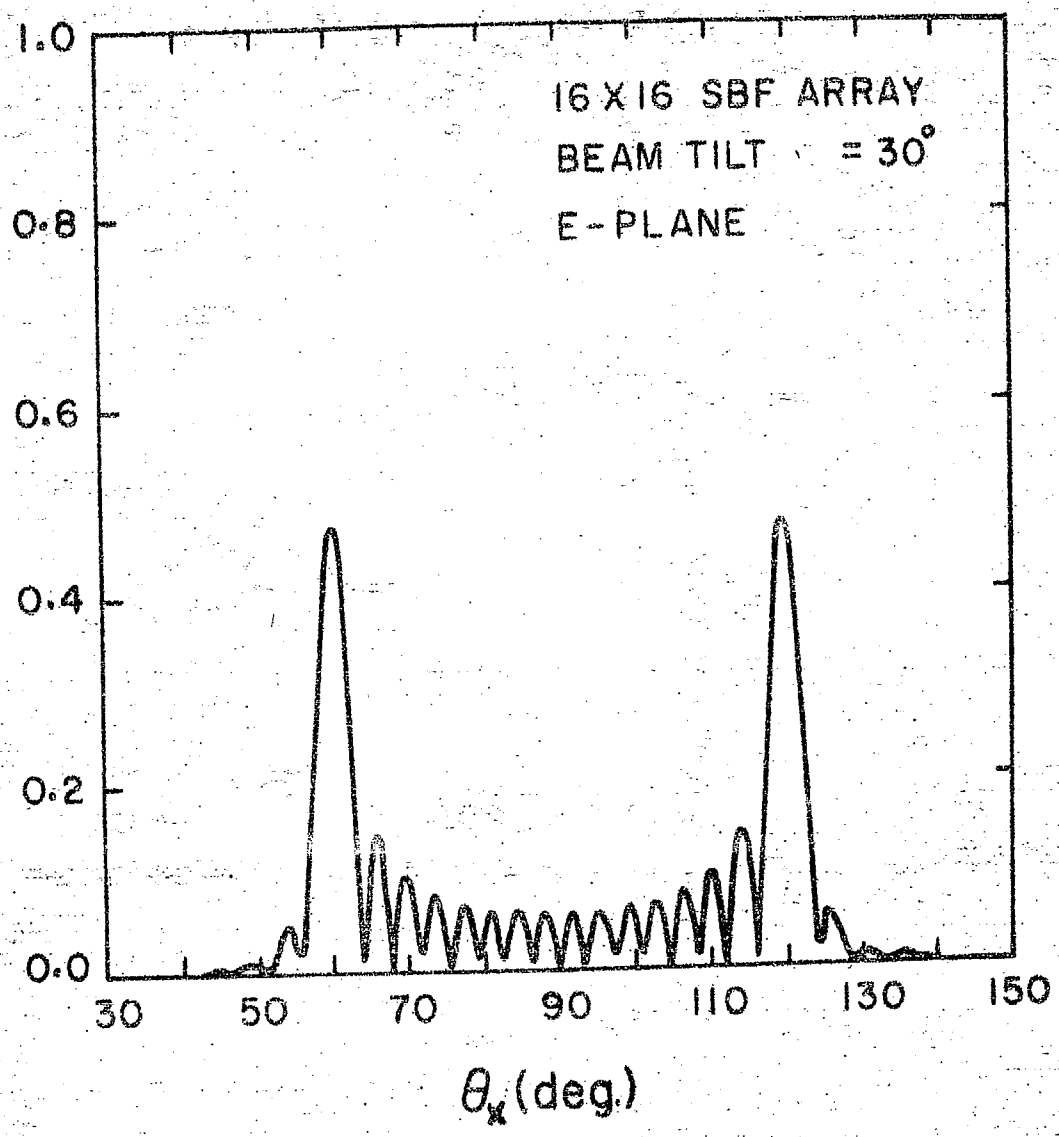

Fig. 13: Normalised radiation pattern of a 16 x 16 SBF array in the E-plane for beam tilt angle = 30°.